U.S. DEPARTMENT OF THE INTERIOR

GEOLOGICAL SURVEY

Petrochemistry of Rocks from the Mohon Mountains Volcanic Field, Yavapai and Mohave Counties, Arizona

By

L. David Nealey[1], A. Wesley Ward[1], Ardit J. Bartel[2], Davison V. Vivit[3], and Roy J. Knight[2]

U.S. Geological Survey

[1]Flagstaff, Arizona, [2]Lakewood, Colorado, and [3]Menlo Park, California

Open-File Report 86-423

List of Figures

List of Tables

INTRODUCTION

This report presents geochemical data from samples of volcanic rocks in the Mohon Mountains volcanic field in west-central Arizona. The Mohon Mountains volcanic field lies east of the Aquarius Mountains (fig. 1) between lat 34° 30' and 35° 10' N, and long 113° 00' and 113° 30' W. The Mohon Mountains are in the Transition Zone between the Colorado Plateau and the Basin and Range Provinces. On the east flank of the Aquarius Mountains, Cenozoic volcanic rocks rest directly on Precambrian basement. Volcanic rocks rest on Paleozoic rocks east of the Mohon Mountains (Fuis, 1973; Goff and others, 1983; Arney and others, 1985).

The volcanic terrane east of the Aquarius Mountains includes at least five silicic centers: the Aquarius Mountains (Goff and others, 1979); Mount Hope (Simmons, 1986), Mohon Mountains, Red Canyon, and an unnamed silicic center in Burro Creek, southeast of the Mohon Mountains. These silicic centers and the surrounding basaltic terrane form the Mohon Mountains volcanic province. The Mohon Mountains volcanic field is located on a line that passes through several late Cenozoic bimodal basalt-rhyolite volcanic fields: Mount Floyd; Kaiser Springs; and Castaneda Hills (Nealey, 1980; Suneson and Lucchitta, 1983; Bush, 1986; Moyer, 1986).

The Mohon Mountains field developed in at least three stages: in the oldest, poorly to moderately bedded pyroclastic flow breccias formed; in the second stage, silicic lavas extruded from dikes and domes around the central vent area; and in the third stage, basaltic dikes intruded the silicic pile, and basaltic cinder cones and associated flows were emplaced peripheral to the silicic pile.

The age of volcanism in the Mohon Mountains is poorly known; only a few samples from the area have been dated. Simmons (1986) reports a whole-rock K-Ar age of 8.5±0.5 Ma on a rhyolite from the Mount Hope dome and a whole-rock K-Ar age of 8.0±0.9 Ma on a basalt flow from north of Mount Hope. The Peach Springs Tuff (17 Ma; Damon and others, 1966), a regional stratigraphic marker in western Arizona and southeastern California, crops out north of the Mohon Mountains. Young and Brennan (1974) stated that the Peach Springs Tuff underlies basalt flows of the Mohon Mountains volcanic field.

COMPOSITION OF VOLCANIC ROCKS

Eighteen rock samples from the Mohon Mountains field were analyzed by X-ray fluorescence and instrumental neutron-activation. The major-element rock analyses are presented in table 1. Sample locations are given in table 2. FeO and Fe_2O_3 were calculated using the equation $FeO/Fe_2O_3 = 9.027 - 0.921 \times SiO_2$ (Wolfe, 1983). CIPW norms were calculated volatile free. Trace-element analyses are given in tables 2 and 3.

The petrography of the Mohon Mountains lavas is similar to that of many upper Cenozoic volcanic rocks in the region. Basaltic lavas contain phenocrysts of olivine, augite, and plagioclase in a matrix of opaque oxides, sanidine, apatite, and glass. Andesite is composed of plagioclase, sanidine, clinopyroxene, orthopyroxene, quartz, opaque oxides, and apatite. Dacitic to rhyolitic lavas contain phenocrysts of plagioclase, quartz, sanidine, hornblende, biotite, orthopyroxene, clinopyroxene, and apatite.

Several basalt flows in the Mohon Mountains volcanic field contain ultramafic, mafic, and crustal xenoliths, and mafic and felsic megacrysts. Xenoliths are heterogeneously distributed within xenolith-bearing flows. The inclusions attain maximum dimensions of 16 cm. The size range is typical of xenoliths in basaltic rocks in central Arizona (Wilshire and others, 1985). The megacryst suite includes clinopyroxene, plagioclase, amphibole, magnetite, and olivine. Black clinopyroxene is the dominant megacrystal phase, followed by plagioclase and amphibole. Magnetite and olivine megacrysts are rare. These same phases are found in basaltic rocks in other Arizona volcanic fields (Nealey, 1980; Suneson and Lucchitta, 1983; Wilshire and others, 1985).

Amphibole and plagioclase megacrysts contain numerous parallel-aligned tubular voids that may have formed by the exsolution of gases from the magma. They suggest that the megacrysts formed at relatively shallow depths.

Volcanic rocks of the Mohon Mountains volcanic field range in composition from basalt to low-silica rhyolite (fig. 2). Mafic volcanic rocks are alkalic basalt and olivine tholeiite in the classification scheme of Wilkinson (1967). Silica-variation diagrams for the Mohon Mountains volcanic suite are presented in figure 3. With the exception of the P_2O_5, K_2O, TiO_2, and Al_2O_3 plots, the major elements are strongly to moderately correlated with silica (fig. 3). Alkalic basalts (samples NSP-2A and NBM-6) are enriched in TiO_2 and P_2O_5 and depleted in CaO compared to the olivine tholeiites (samples NSP-4B, WPK-1, NBM-12, and NPPB-9). The variation diagrams suggest that the olivine tholeiites are not genetically related to the alkalic basalts, andesites, and dacites. However, if the tholeiites represent higher degrees of partial melting, the olivine tholeiites and alkalic basalts may have been derived from the same parent magma. Basalts of the Mohon Mountains volcanic field plot above and below the MacDonald-Katsura line which separates alkalic from tholeiitic basalts in the Hawaiian Islands (fig. 4).

On ternary plots of total alkalies, magnesium, and iron ($Fe_2O_3 = TiO_2 + 1.5$), the Mohon Mountains suite shows no evidence of iron enrichment with increasing differentiation. When alkalic rocks are ignored, the olivine tholeiites straddle the line used by Irvine and Baragar (1971) to distinguish tholeiitic from calc-alkalic rocks. The alkalic basalts lie within the calc-alkalic field of Irvine and Baragar. Andesites and dacites straddle the line that defines the trend in the Cascade volcanic province (fig. 5).

Mohon Mountains tholeiites are depleted in Rb, Sr, and Ba compared to the alkali basalts, intermediate rocks, and silicic rocks (figs. 6 and 7; table 3). They are also depleted in Nb, Hf, Ta, and Zr and enriched in Cr and Ni compared to the alkali basalts. The basalts as a group are mildly enriched in light rare-earth elements compared to heavy rare-earth elements (fig. 8); chondrite-normalized La/Yb ratios [(La/Yb_N)] range from 4.5 to 9.2.

Compared to average within-plate basalts of Pearce (1982), the Mohon Mountains basalts are intermediate between the average within-plate tholeiite and the average within-plate alkalic basalt. Mohon Mountains tholeiites are chemically very similar to average within-plate tholeiite, but the alkalic basalts are depleted in trace elements compared to average within-plate alkalic basalt. Chromium is especially low in the Mohon Mountains alkalic basalts compared to average 536-ppm in within-plate alkalic basalt (Pearce, 1982).

The intermediate and silicic rocks contain unusually high concentrations of several trace elements. There is a four-fold increase in Ba content from basalt to andesite, then decreases with continuing differentiation to rhyolite. The Hf concentration increases by a factor of four from olivine basalt to andesite; then drops by about 50 percent in the dacitic lavas. U and Th contents also increase from basalt to andesite. Sr is especially high for differentiated rocks (as much as 2150 ppm). The trace elements Sc, Zn, Ni, and Co are negatively correlated, and Cs and Sb are positively correlated with SiO_2. Mafic and silicic rocks of the suite plot in distinct fields on Zr/Nb versus SiO_2 diagrams. The differentiated rocks show light rare-earth element enrichment patterns (fig. 8), with $(La/Yb)_N$ ranging from 18.5 to 32.7. The most evolved sample (WPK-6) is depleted in all trace elements except Sb, compared to the least evolved member of the high potassium group (basaltic andesite, sample NPK-25I).

The Mohon Mountains volcanic suite plots near the Th apex on plots of Th-Ta-Hf/3 (fig. 9). The analyses fall in the within-plate (WPV), enriched mid-ocean ridge basalt (E-MORB), convergent-plate margin (CPM) fields of Wood and others (1979). With increasing differentiation, from basalt to andesite, the analyses plot closer to the Th apex. Samples in the andesite to dacite range however plot toward the average composition for Precambrian granitic basement rocks in central Arizona. This pattern suggests that the silicic lavas are related to the Precambrian basement of central Arizona (C.M. Conway and C.T. Wrucke, written commun., 1985). The silicic rocks may represent either anatectic melts, the products of magma mixing, or fractionated melts that were contaminated by crustal material, or some combination.

Basalt collected north of Mount Hope has a strontium isotopic composition of 0.70388, and flow-banded rhyolite from Mount Hope has a Sr isotopic composition of 0.70491 (Simmons, 1986). These values are characteristic of Cenozoic volcanic rocks in Arizona (Leeman, 1982). The higher ratio for the Mount Hope rhyolite may be caused by crustal contamination or anatexis.

REFERENCES

Arney, Barbara, Goff, Fraser, and Eddy, A.C., 1985, Chemical, petrographic, and K-Ar age data to accompany reconnaissance geologic strip map from Kingman to south of Bill Williams Mountain, Arizona: Los Alamos National Laboratory Report LA-10409-HDR UC-66a, 26 p.

Bush, M.M., 1986, The geology of Round Mountain, a bimodal volcanic field in northwest Arizona: State University of New York at Buffalo, M.S. thesis, 110 p.

Carmichael, I.S.E., Turner, F.J., and Verhoogen, John, 1974, Igneous Petrology: New York, McGraw-Hill Book Company, 739 p.

Damon, P.E., 1966, compiler, Correlation and chronology of ore deposits and volcanic rocks: U.S. Atomic Energy Commission Contract AT(11-1)-689, Annual Progress Report, COO-689-76, Tucson, University of Arizona, Geochronology Laboratory, 250 p.

Fuis, G.S., 1973, The geology and mechanics of formation of the Fort Rock Dome, Yavapai County, Arizona: Pasadena, California Institute of Technology, Ph.D. dissertation, 278 p.

Goff, F.E., Arney, B.H., Aiken, Carlos, West, F.G., and Eddy, A.C., 1979, Preliminary evaluation of the Aquarius Mountains Hot Dry Rock geothermal prospect, Arizona: Geothermal Resources Council, Transactions, v. 3. p. 257-260.

Goff, F.E., Eddy, A.C., and Arney, B.H., 1983, Reconnaissance geologic map from Kingman to south of Williams, Arizona: Los Alamos National Laboratory Report La-9202-MAP, scale 1:48,000.

Hanson, G.N., 1980, Rare earth elements in petrogenetic studies of igneous systems: Annual Reviews of Earth and Planetary Science, v. 8, p. 371-406

Irvine, T.N., and Baragar, W.R.A., 1971, A guide to the chemical classification of the common volcanic rocks: Canadian Journal of Earth Sciences, v. 8, p. 523-548.

Leeman, W.P., 1982, Tectonic significance of strontium isotopic variations in Cenozoic volcanic rocks from the western United States: Geological Society of America Bulletin, v. 93, p. 487-503.

MacDonald, G.A. and Katsura, T., 1964, Chemical composition of Hawaiian lavas: Journal of Petrology, v. 5, p. 82-133.

Moyer, T.C., 1986, The Pliocene Kaiser Spring (Arizona) bimodal volcanic field: geology, geochemistry, and petrogenesis: Tempe, Arizona State University, Ph. D. dissertation, 312 p.

Nealey, L.D., 1980, The geology of Mount Floyd and vicinity, Coconino County, Arizona: Flagstaff, Northern Arizona University, M.S. thesis, 144 p.

Pearce, J.A., 1982, Trace element characteristics of lavas from destructive plate boundaries, in R. S. Thorpe, ed., Andesites: Orogenic Andesites and Related Rocks: New York, John Wiley and Sons, p. 525-548.

Peccerillo, A., and Taylor, S.R., 1976, Geochemistry of Eocene calc-alkaline volcanic rocks from the Kastamonu area, northern Turkey: Contributions to Mineralogy and Petrology, v. 58, p. 63-81.

Pierce, H.W., 1986, Paleogeographic linkage between Arizona's physiographic provinces, in Beatty, Barbara, and Wilkinson, P.A.K., 1986, Frontiers in Geology and Ore Deposits of Arizona and the Southwest: Arizona Geological Society Digest, v. 16, p. 74-82.

Simmons, A.M., 1986, The geology of Mount Hope, a volcanic dome in the Colorado Plateau-Basin and Range Transition Zone, Arizona: State University of New York at Buffalo, M.S. thesis, 156 p.

Suneson, N.H., and Lucchitta, Ivo, 1983, Origin of bimodal volcanism, southern Basin and Range Province, west-central Arizona: Geological Society of America Bulletin, v. 94, p. 1005-1019.

Wilkinson, J.F.G., 1967, The petrography of basaltic rocks, in Hess, H.H., and Poldervaart, Arie, eds., Basalts: New York, Wiley and Sons, p. 163-214.

Wolfe, E.W., 1983, Geochemical map of the Arnold Mesa Roadless area, Yavapai County, Arizona: U.S. Geological Survey Miscellaneous Investigations Map MF-1577-C, scale 1:24,000.

Wood, D.A., Joron, J-L., and Treuil, M., 1979, A reappraisal of the use of trace-elements to classify and discriminate between magma series erupted in different tectonic settings: Earth and Planetary Science Letters, v. 45, p. 326-336.

Young, R.A., and Brennan, W.J., 1974, Peach Springs Tuff: Its bearing on structural evolution of the Colorado Plateau and development of Cenozoic drainage in Mohave County, Arizona: Geological Society of America Bulletin, v. 85, p. 83-90.

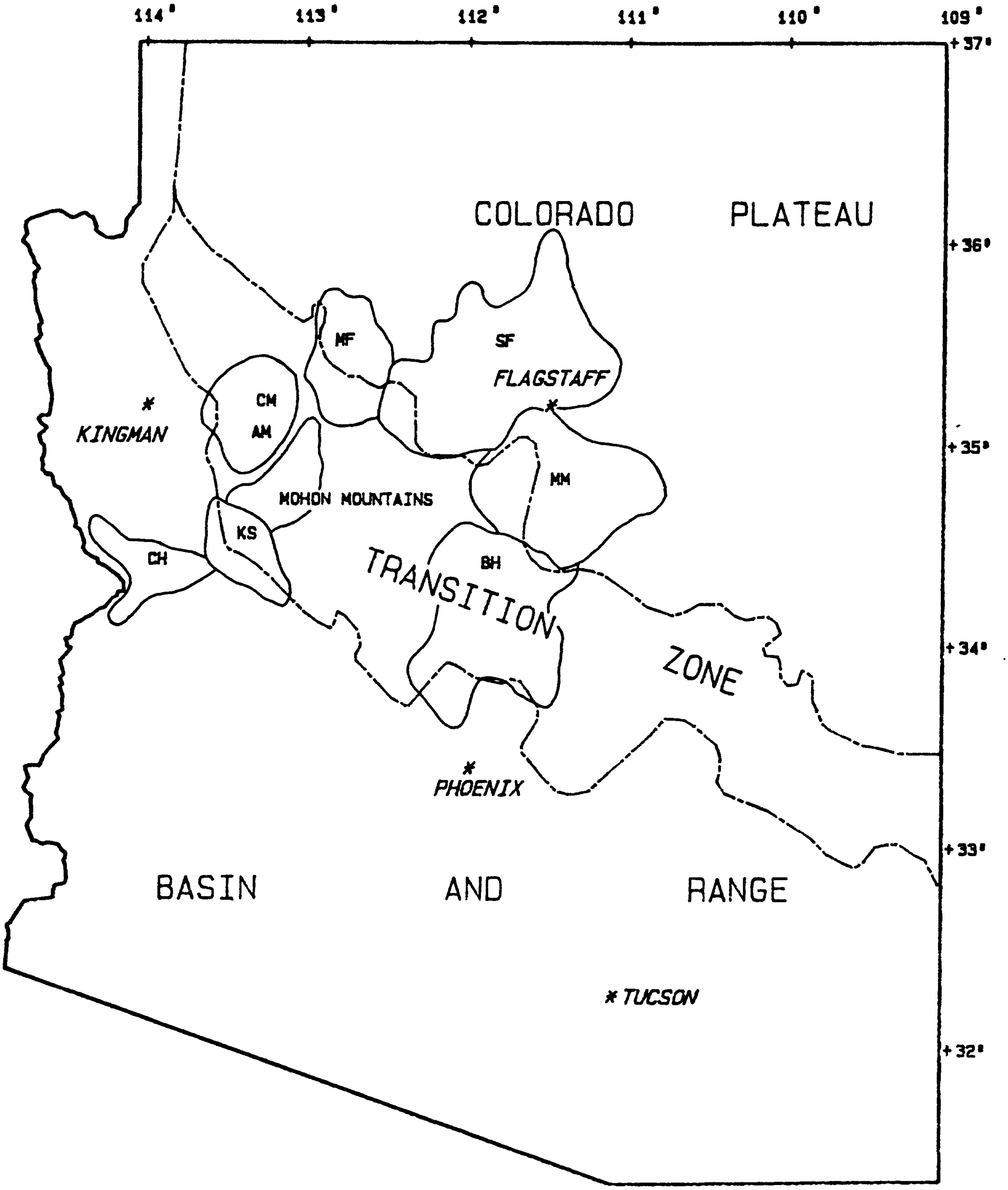

Figure 1. Index map showing the location of the Mohon Mountains volcanic field and other late Cenozoic volcanic fields in Arizona. Tectonic provinces after Pierce (1986). AM = Aquarius Mountains, KS = Kaiser Springs, CH = Castaneda Hills, BH = Black Hills, SF = San Francisco, and MF = Mount Floyd.

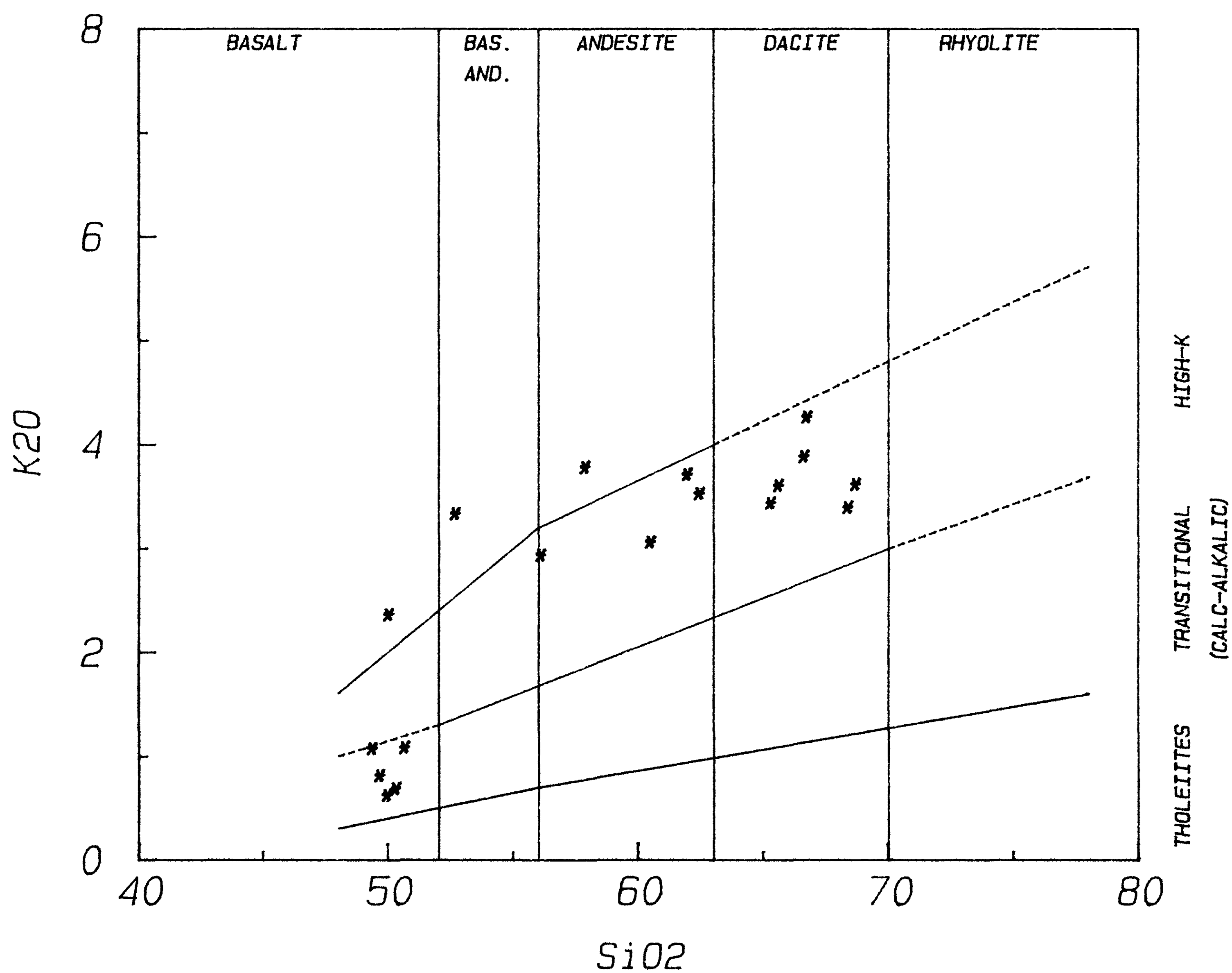

Figure 2. Potassium-silica diagram, Mohon Mountains volcanic suite. Nomenclature after Peccerillo and Taylor (1976). Values in weight percent, adjusted water-free. BAS. AND. = basaltic andesite.

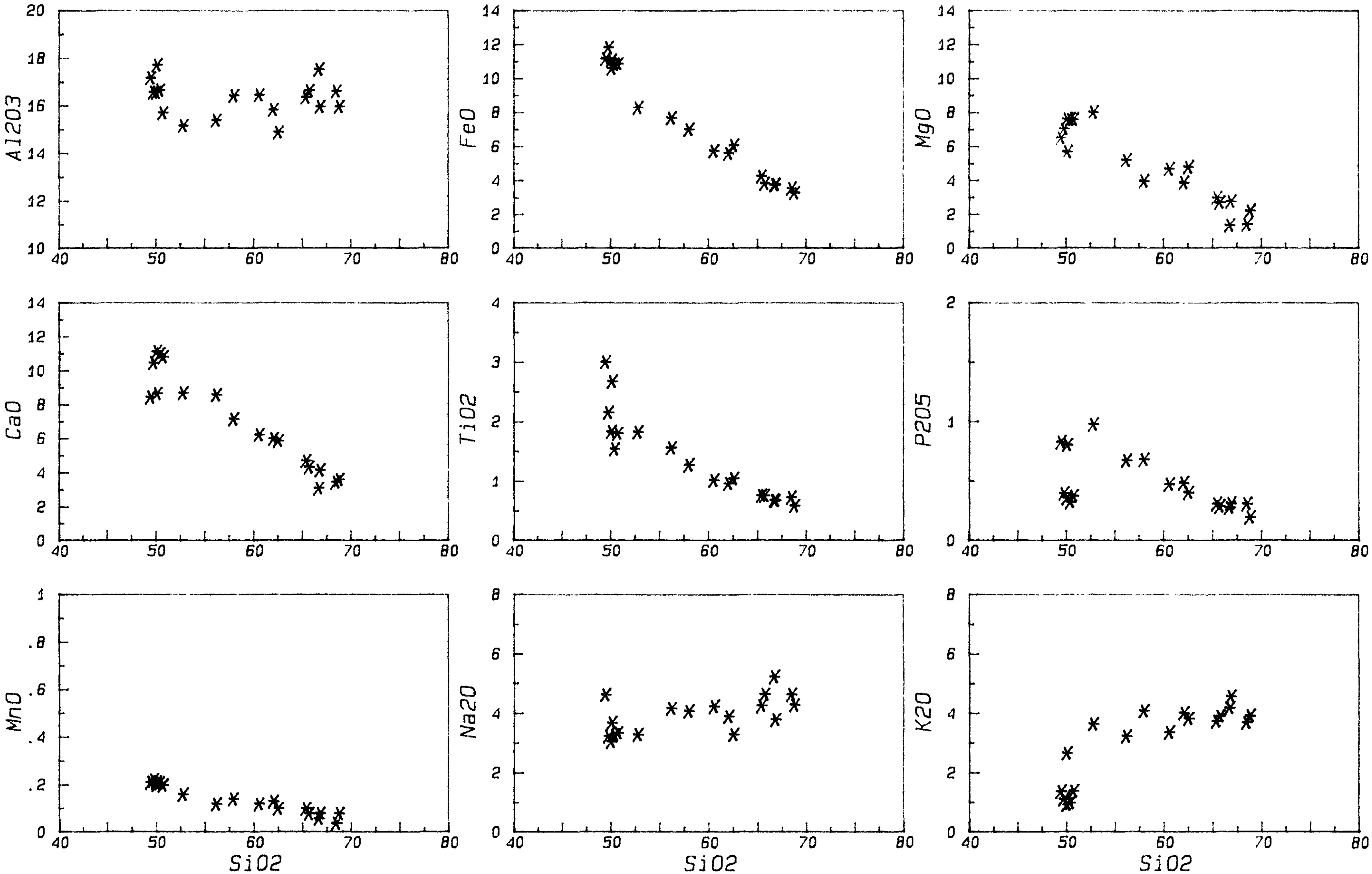

Figure 3. Silica variation diagram, Mohon Mountain volcanic suite. Values in weight percent, adjusted water-free.

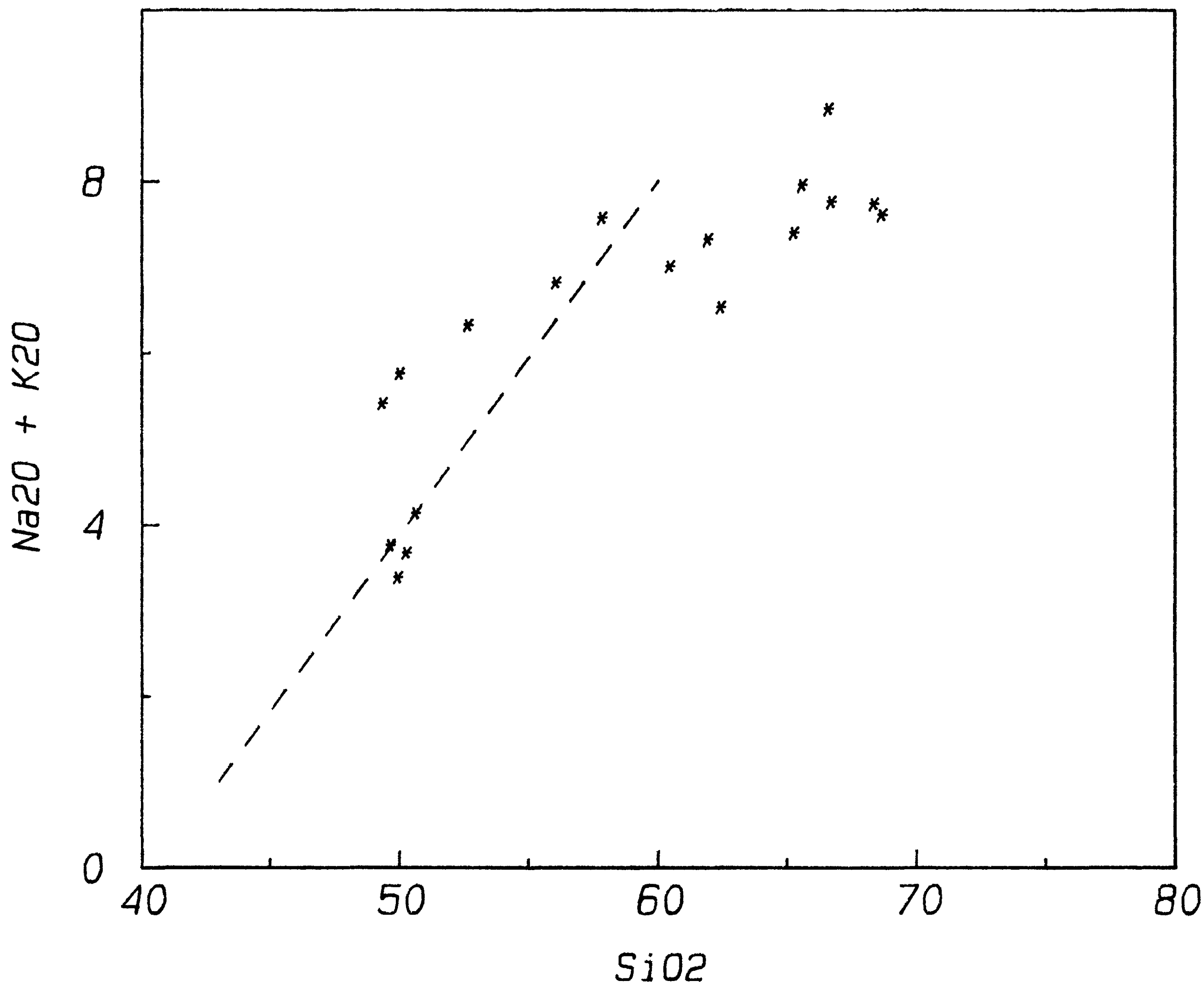

Figure 4. Alkali-silica diagram, Mohon Mountains volcanic suite. Dashed line separates alkalic from tholeittic lavas in the Hawaiian Islands (after Macdonald and Katsura, 1964). Values in weight percent, adjusted water-free.

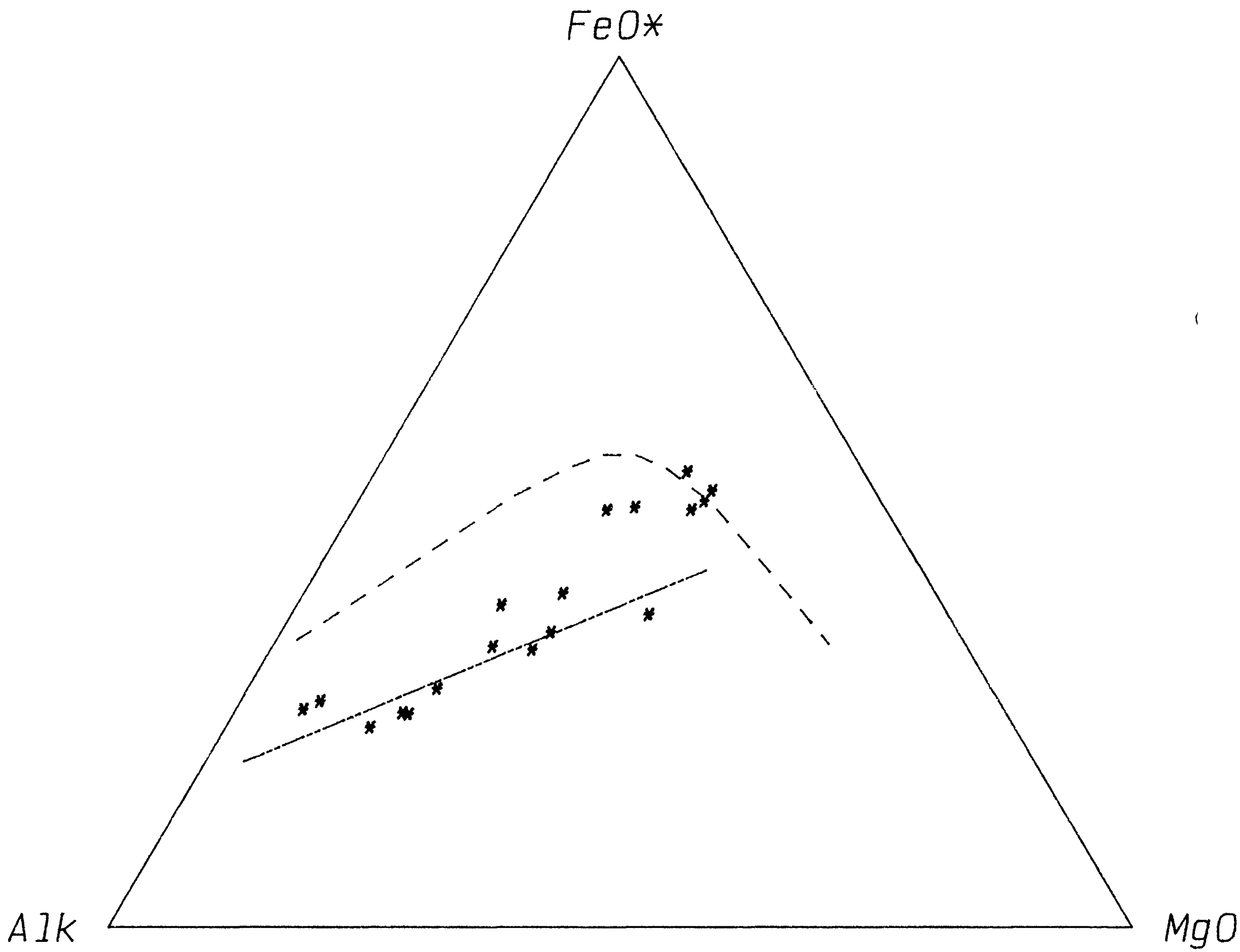

Figure 5. Alkali-magnesium-iron diagram, Mohon Mountains volcanic suite. Total iron (FeO*) adjusted so that Fe_2O_3 equals TiO_2 + 1.5 weight percent. Dashed curve is proposed boundary between tholeiitic (above) and calc-alkalic rock series (below) (Irvine and Baragar, 1971). Dot-dash line is trend of Cascade volcanic province (Carmichael and others, 1974).

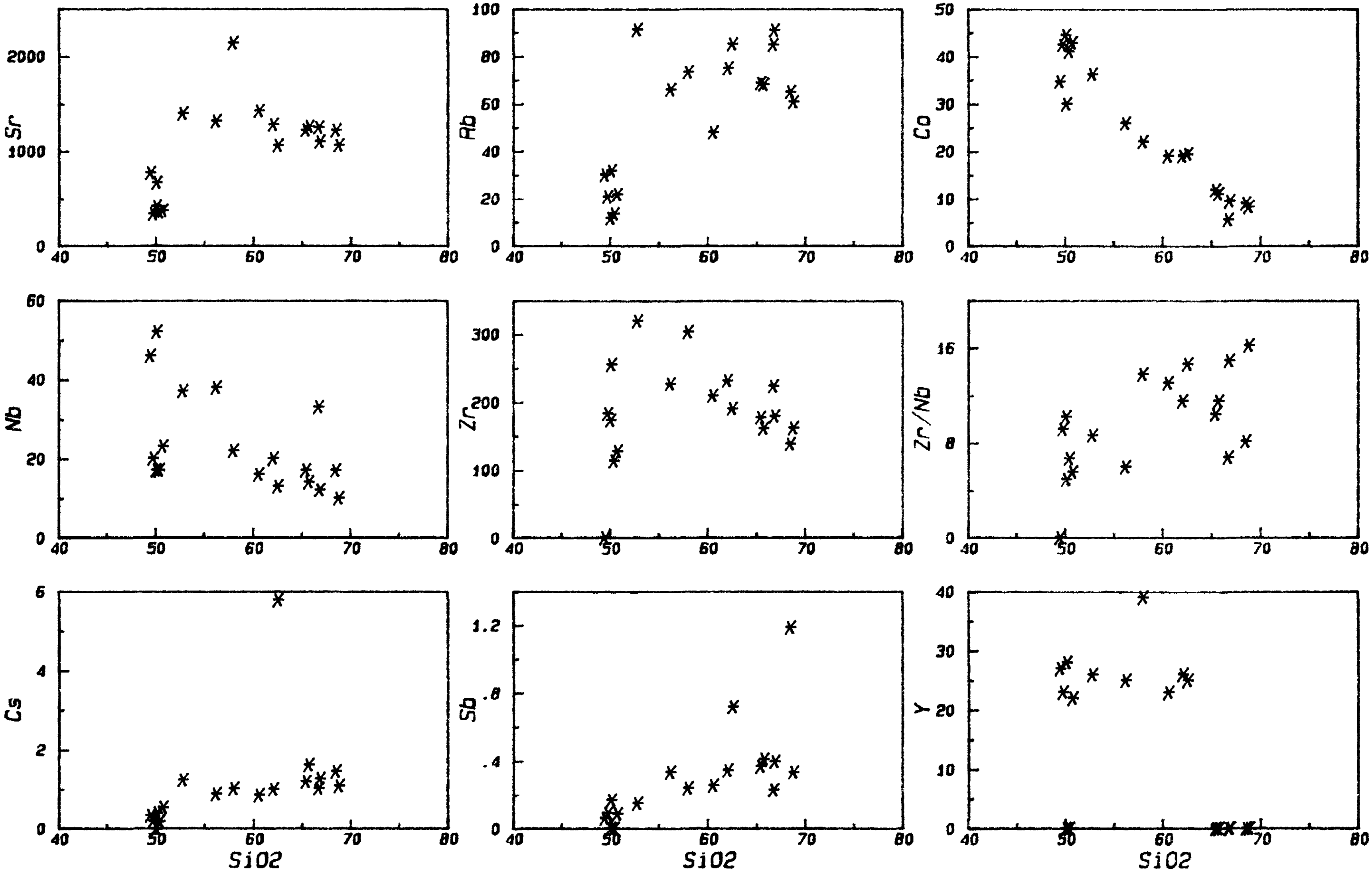

Figure 6. Variation diagrams of Th, U, Sc, Hf, Ta, Zn, Cr, Ni, and Ba for the Mohon Mountains volcanic suite. Trace element concentrations below detection limit are plotted as zero. Silica in weight percent, adjusted water-free. Trace elements in parts per million.

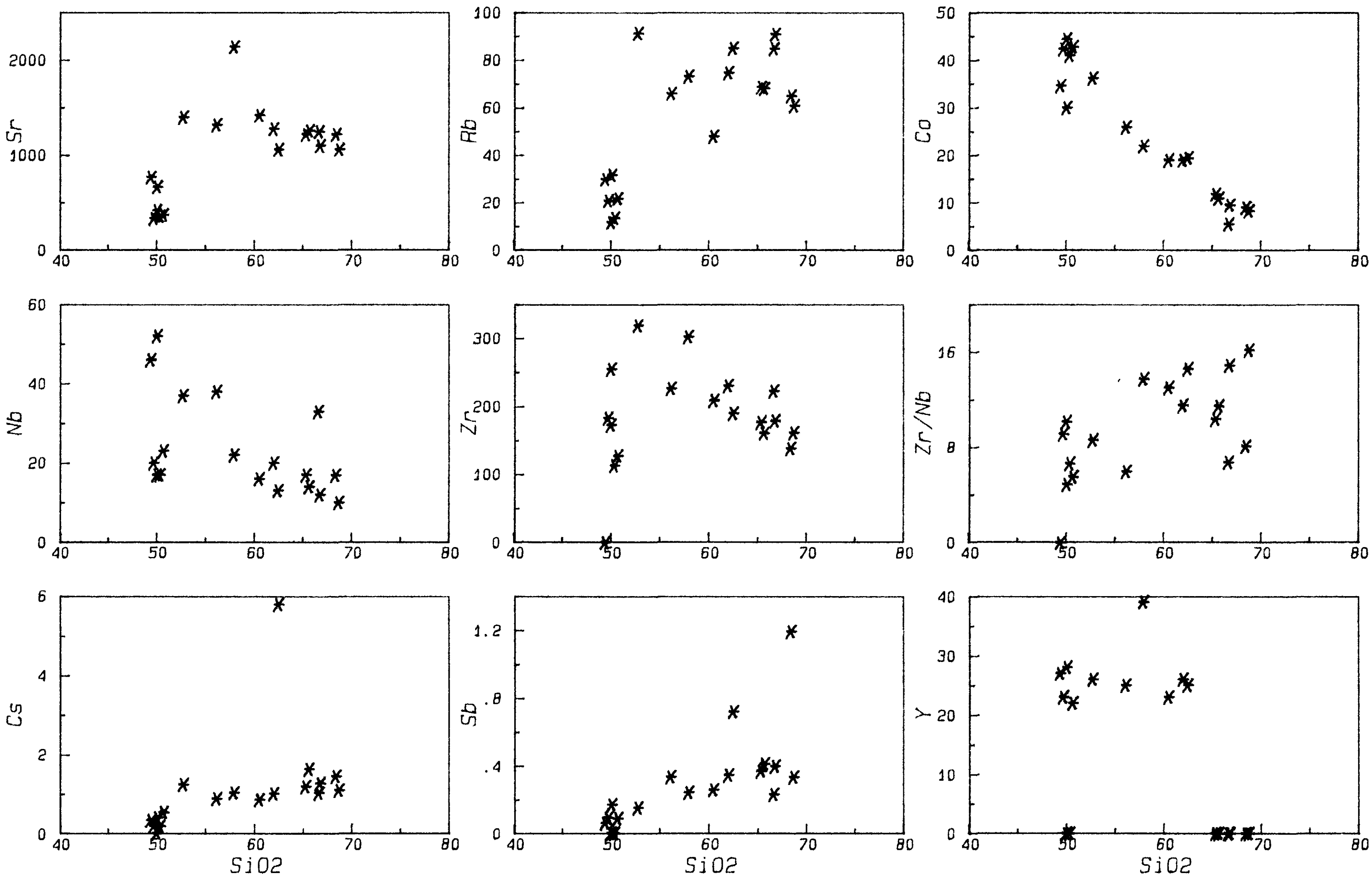

Figure 7. Variation diagrams of Sr, Rb, Co, Nb, Zr, Zr/Nb, Cs, Sb, and Y for the Mohon Mountains volcanic suite. Trace-element concentrations below detection limit are plotted as zero. Silica in weight percent, adjusted water-free. Trace elements in parts per million.

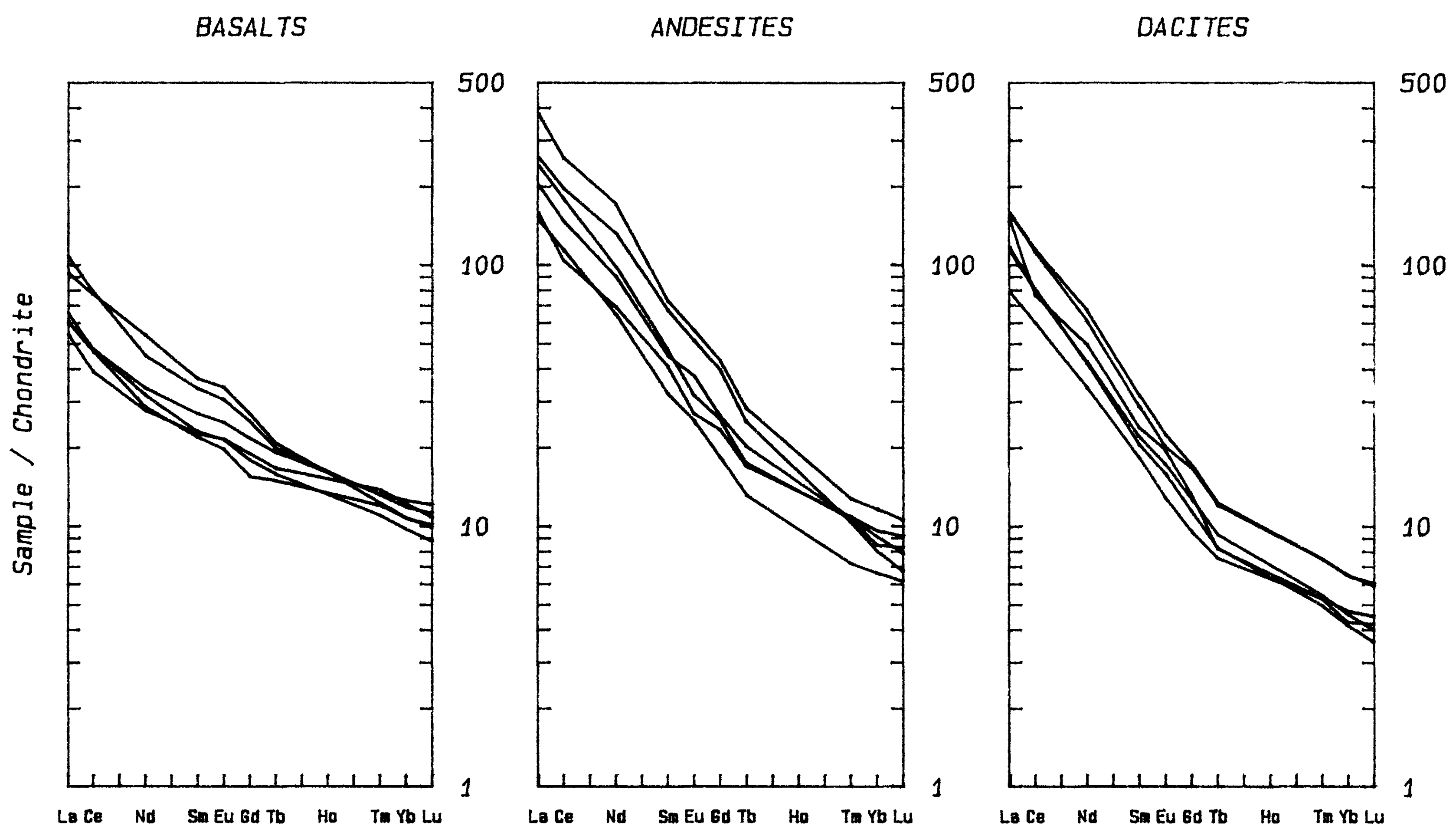

Figure 8. Chondrite-normalized rare-earth element patterns, Mohon Mountains volcanic suite. Chondritic values from Hanson (1978).

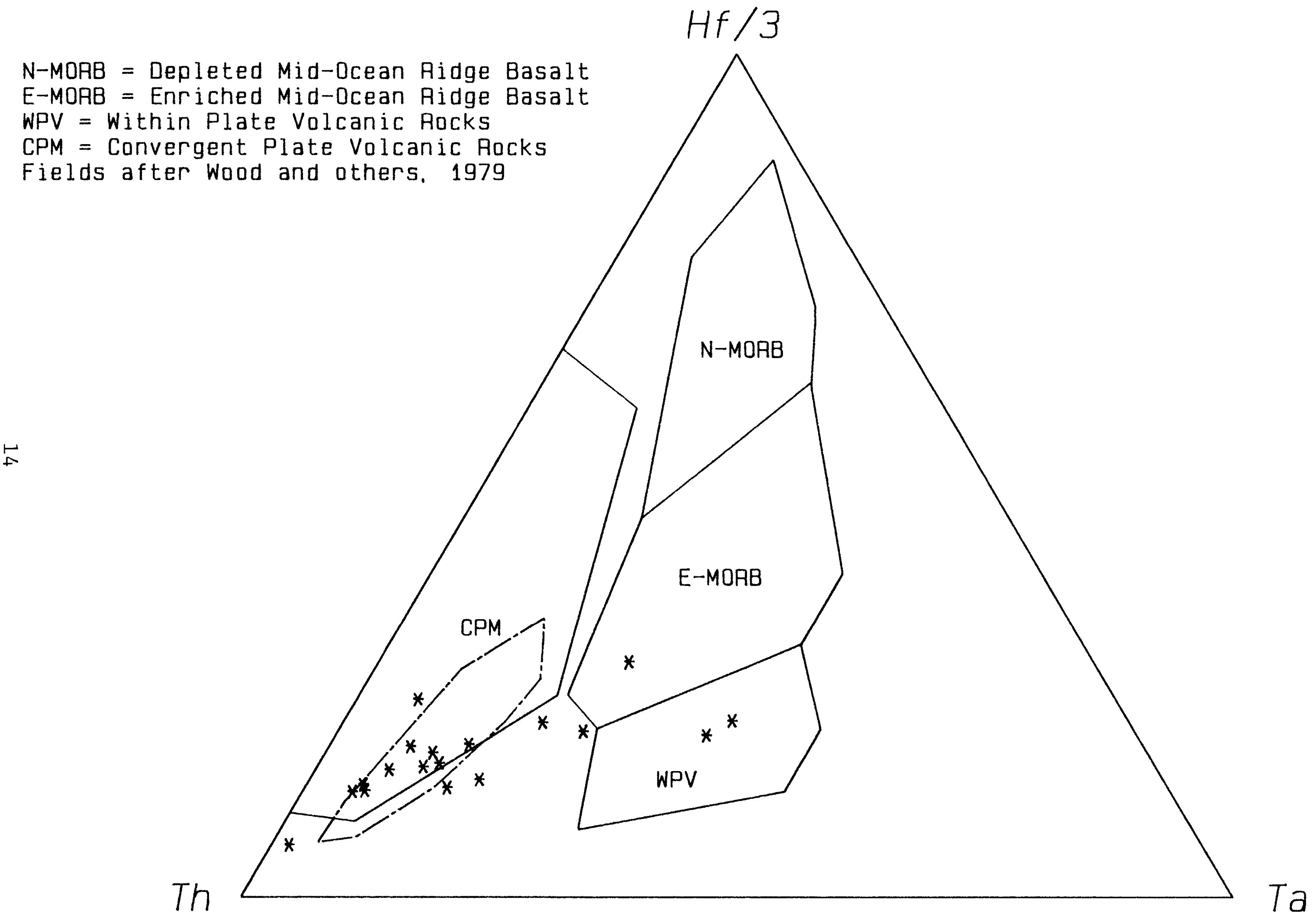

Figure 9. Ternary plot of Th, Ta, and Hf, Mohon Mountains volcanic suite. Dashed line is field of Precambrian rocks in central Arizona (C. Conway and C. Wrucke, U. S. Geological Survey, written communication).

Table 1.--Major-element analyses and CIPW norm calculations of Mohon Mountains volcanic rocks.
[Values in weight percent]

Sample No.	NSP-2A	NSP-2B	NSP-2C	NSP-4B	WPK-1	WPK-4	WPK-5	WPK-6	NBM-7
SiO_2	48.7	64.2	56.2	49.0	50.0	58.7	54.1	66.5	63.7
Al_2O_3	16.9	15.0	15.6	15.9	16.2	15.6	14.5	15.1	15.8
$FeTO_3$	10.9	3.47	7.01	11.5	11.4	5.64	7.69	2.98	3.58
MgO	5.04	2.16	3.37	6.97	7.04	4.04	4.53	1.63	2.13
CaO	7.92	3.49	6.46	10.4	10.4	5.51	7.77	2.96	3.69
Na_2O	3.30	3.36	3.68	2.70	2.96	3.83	3.74	3.86	4.22
K_2O	2.31	4.11	3.68	0.62	0.69	2.98	2.84	3.51	3.51
TiO_2	2.46	0.50	1.09	1.65	1.38	0.84	1.36	0.42	0.59
P_2O_5	0.71	0.23	0.59	0.28	0.25	0.39	0.58	0.12	0.21
MnO	0.16	0.04	0.10	0.17	0.17	0.08	0.08	0.04	0.04
LOI 900°	1.75	3.06	1.61	1.46	0.25	1.95	2.32	2.42	1.74
Q	0	18.51	3.20	0	0	7.72	0.71	21.66	14.82
C	0	0	0	0	0	0	0	0	0
or	14.00	25.22	22.37	3.73	4.10	18.13	17.38	21.41	21.34
ab	28.65	29.53	32.04	23.26	25.17	33.36	32.78	33.71	36.75
an	25.11	14.24	15.62	29.97	29.02	17.06	14.90	13.94	14.20
ne	0	0	0	0	0	0	0	0	0
wo	4.36	0.91	5.59	8.64	8.84	3.53	8.81	0.17	1.35
en	3.82	5.59	8.64	12.83	10.85	10.36	11.69	4.19	5.46
fs	3.12	3.44	7.26	9.12	7.80	5.80	7.80	2.89	3.40
fo	6.35	0	0	3.40	4.74	0	0	0	0
fa	5.70	0	0	2.66	3.75	0	0	0	0
mt	2.42	1.02	1.76	2.54	2.53	1.48	1.88	0.91	1.03
il	4.79	0.99	2.13	3.19	2.63	1.64	2.68	0.82	1.15

Analyses by X-ray spectroscopy. Analysts: A. J. Bartel and K. C. Stewart

Table 1 cont.--Major-element analyses and CIPW norm calculations of Mohon Mountains volcanic rocks.

[Values in weight percent]

Sample No.	NBM-12	NBM-16	NPK-25H	NPK-25I	NPK-27	WMP-32	WMP-34	NPPB-9	NBM-6
SiO_2	50.2	60.2	66.5	51.2	65.2	60.1	63.3	49.0	48.4
Al_2O_3	15.2	14.0	15.8	14.4	16.8	15.0	15.5	16.0	16.5
$FeTO_3$	11.4	5.95	3.27	8.39	3.51	5.49	4.03	12.4	11.6
MgO	7.02	4.13	0.86	7.29	0.81	3.27	2.42	6.45	5.89
CaO	10.2	5.15	2.84	7.95	2.51	5.31	4.04	9.82	7.77
Na_2O	3.02	2.89	4.22	2.90	4.85	3.50	3.84	2.90	4.25
K_2O	1.08	3.41	3.31	3.25	3.81	3.61	3.34	0.81	1.06
TiO_2	1.64	0.86	0.56	1.63	0.52	0.79	0.59	1.98	2.80
P_2O_5	0.30	0.32	0.23	0.88	0.20	0.40	0.23	0.32	0.74
MnO	0.16	0.06	<0.02	0.12	0.02	0.09	0.06	0.18	0.17
LOI 900^o	0.14	2.35	2.00	1.21	1.46	1.84	2.02	0.75	0.89
Q	0	13.65	21.86	0	15.22	10.59	16.00	0	0
C	0	0	.68	0	.62	0	0	0	0
or	6.43	20.88	20.10	19.74	22.98	21.97	20.34	4.84	6.38
ab	25.75	25.35	36.69	25.22	41.90	30.50	33.49	24.83	35.36
an	24.91	15.71	12.93	17.14	11.38	14.99	15.66	28.59	23.23
ne	0	0	0	0	0	0	0	0	0.68
wo	10.06	3.59	0	7.30	0	3.94	1.44	7.77	4.63
en	10.27	10.66	2.20	9.51	2.06	8.39	6.21	10.68	2.58
fs	7.12	6.08	2.90	4.29	3.32	5.65	4.01	8.63	1.87
fo	5.15	0	0	6.41	0	0	0	3.91	8.66
fa	3.94	0	0	3.19	0	0	0	3.48	6.90
mt	2.54	1.62	1.00	1.94	1.03	1.48	1.15	2.73	2.54
il	3.14	1.69	1.09	3.18	1.01	1.55	.1.15	3.81	5.42

Analyses by X-ray spectroscopy. Analysts: A. J. Bartel and K. Stewart

Table 2.--Type and location of rock samples, Mohon Mountains volcanic field.

Sample No.	Rock Type	Latitude	Longitude
NSP-2A	Basalt	34°55'50"	113°13'52"
NSP-2B	High-K dacite	34°55'49"	113°13'52"
NSP-2C	High-K andesite	34°55'49"	113°13'52"
NSP-4B	Basalt	34°53'44"	113°14'45"
WPK-1	Basalt	34°49'06"	113°20'32"
WPK-4	High-K andesite	34°48'05"	113°16'45"
WPK-5	High-K andesite	34°48'21"	113°16'56"
WPK-6	High-K dacite	34°48'25"	113°16'59"
NBM-7	High-K dacite	34°50'46"	113°14'38"
NBM-12	Basalt	34°51'28"	113°14'06"
NBM-16	High-K andesite	34°50'53"	113°14'15
NPK-25H	High-K dacite	34°51'20"	113°15'59"
NPK-25I	Basaltic andesite	34°51'20"	113°15'59"
NPK-27	High-K dacite	34°50'28"	113°18'13"
WMP-32	High-K andesite	34°54'40"	113°22'09"
WMP-34	High-K dacite	34°54'42"	113°20'48"
NPPB-9	Basalt	34°50'31"	113°21'17"
NBM-6	Basalt	34°51'12"	113°14'06"

Sample NPK-25I is an inclusion in unit represented by NPK-25H.

Table 3.--Trace-element analyses, Mohon Mountains volcanic suite.

[Values in parts per million]

Sample No.	NSP-2A	NSP-2B	NSP-2C	NSP-4B	WPK-1	WPK-4	WPK-5	WPK-6	NBM-7
*Nb	52	12	22	17	17	16	38	10	14
*Rb	30	92	92	11	15	63	70	62	72
*Sr	675	990	2100	350	414	1250	1225	1050	1050
*Zr	262	210	374	115	117	236	248	170	210
*Y	28	<20	39	<20	<20	23	25	<20	<20
*Cu	52	<20	64	95	83	50	65	20	34
*Ni	70	32	44	118	92	70	132	20	25
*Zn	76	63	92	80	73	74	87	46	50
Ni	79.4	39.2	61.5	119.0	101.0	76.0	128.0	30.6	42.0
Sr	668	1100	2140	417	355	1420	1320	1060	1260
Ba	447	1540	2420	256	373	1340	1640	1470	1500
Co	30.0	9.5	22.0	44.4	41.0	19.0	25.9	8.26	11.0
Cr	136.0	65.3	87.1	312.0	249.0	118.0	332.0	42.3	52.7
Cs	0.39	1.26	1.02	-	0.18	0.85	0.88	1.09	1.62
Hf	5.4	5.1	7.3	2.7	2.5	4.7	5.5	4.2	4.2
Rb	31.7	90.9	73.3	12	13.5	47.9	66.0	60.8	68.1
Sb	0.17	0.40	0.24	-	-	0.26	0.33	0.33	0.41
Ta	3.50	0.72	0.96	0.86	0.64	0.72	2.23	0.36	0.95
Th	4.1	10.3	15.9	2.5	3.1	6.5	9.0	4.1	6.6
U	1.0	2.0	2.7	0.5	0.5	1.0	1.9	1.0	1.5
Zn	90	72	113	-	92	102	108	75	72
Zr	255	179	303	<170	113	209	227	160	161
Sc	17.8	6.9	14.7	33.3	31.0	10.2	18.5	5.7	6.1
La	34.1	49.7	119.0	17.2	19.1	46.9	63.9	24.8	35.8
Ce	63.3	90.6	208.0	31.4	37.7	92.3	119.0	48.6	63.8
Nd	26.7	36.3	102.0	16.4	16.9	38.3	53.4	20.1	25.2
Sm	6.41	5.50	13.9	4.31	4.17	6.13	8.59	3.49	4.20
Eu	2.12	1.40	3.90	1.50	1.37	1.76	2.61	0.89	1.20
Gd	6.48	4.30	11.1	4.88	3.99	4.72	6.77	2.45	3.25
Tb	0.93	0.56	1.32	0.78	0.70	0.61	0.94	0.35	0.43
Tm	-	0.22	0.38	0.41	0.36	0.22	-	0.15	0.16
Yb	2.44	1.34	2.40	2.51	2.21	1.37	1.89	0.88	0.95
Lu	0.36	0.19	0.34	0.35	0.33	0.20	0.25	0.14	0.13

* Analyses by x-ray spectroscopy. All other elemental analyses by instrumental neutron-activation analysis. Analysts: D.V. Vivit, J.R. Budahn, R. J. Knight, and D. M. McKown. Dashes indicate that the element was not detected.